IEEE Access
Multidisciplinary | Rapid Review | Open Access Journal

Received February 24, 2020, accepted March 20, 2020, date of publication April 6, 2020, date of current version April 30, 2020.

Digital Object Identifier 10.1109/ACCESS.2020.2985736

Performance and Correlations of Weighted Circuit Networks

TINGYUAN NIE, (Member, IEEE), BO FAN, ZUYUAN ZHU, AND LIJIAN ZHOU
School of Information and Control Engineering, Qingdao University of Technology, Qingdao 266033, China

Corresponding author: Tingyuan Nie (tynie@qut.edu.cn)

This work was supported by the National Natural Science Foundation of China under Grant 61572269.

ABSTRACT The patterns and evolution of man-made complex networks have been topics of interest in recent years. Herein, we define appropriate metrics to quantify the correlations between circuit performance and the complex network characteristics regarding the physical design of circuits. The experimental results show that circuit performance differs due to the optimization tools, both at placement and routing. The strength of the correlations with placement design follows the order of average distance, betweenness, average strength, and the clustering coefficient; the strength of the correlations with layout design follows the order of betweenness, average strength, average distance, and the clustering coefficient. The correlation between performance and betweenness has been further strengthened after routing and presents a remarkable difference in comparison with other characteristic parameters, which indicates its significance to the dynamic correlation with circuit performance.

INDEX TERMS Weighted complex network, circuit design, correlation, performance, complex network characteristics.

I. INTRODUCTION

With the enormous progress of semiconductor manufacturing technology, VLSI (very-large-scale integration circuit) design has achieved rapid development following Moore's Law. Billions of components are integrated into a single chip to improve the performance, which substantially increases the design complexity simultaneously [1]. The cost, quality and predictability of IC (integration circuit) design have become intertwined challenges to the ability of designers to exploit advances in underlying patterning, device and integration technologies [2]. The physical design is a crucial stage for the resulting circuit performance. Conventional optimization tools may not be efficient enough to solve such problems, and considerable efforts are devoted to the development of new methods and algorithms for improving the performance of EDA tools [3].

As a subject that explains the phenomena and complexity of existing systems, complex networks have experienced booming interest in recent years. The study of complex networks spans a multitude of research fields from natural science to social science [4]–[11]. In recent decades, theories and growth models for explaining phenomena in the optimization of complex networks have been established [12]–[14]. Especially, research on robustness and controllability of the network indicate the close correlation to the properties of complex networks (such as scale-free, small-world, etc.) [15]–[19].

As a special category of network, man-made networks are typically designed for distribution of some commodity or resource. The studied distribution networks include airline networks [20], [21], railways [22], [23], power grids [12], [24], electronic circuits [25], etc.

The electronic circuit can be viewed as a network in which components are considered as vertices and wires between components are considered as edges. The evolution of electronic circuits underwent transitions from analog circuits to digital circuits, then to high integration. Early research showed that both analog and digital circuits exhibit small world behaviors [25]. Later, Teuscher et al. demonstrated that the chip system with small-world characteristics can adapt to scale growth and presents superior performance and robustness with respect to regular structured chips [26], [27]. Oshida et al. investigated the network-on-chip (NoC) performance with different structures through dynamic flow analysis. They found that the NoC architecture constructed with the topology in which hubs mostly connect to lower-degree nodes achieves short latency and low packet loss ratio [28].

The associate editor coordinating the review of this manuscript and approving it for publication was Gang Mei.

Zhan et al. devised a multi-layered design architecture to capture favorable characteristics of biological mechanisms for the application of electronic circuit design. This demonstrates that utilizing biological mechanisms for engineering design is a promising approach for building intelligent systems [29]. To identify the infringement of intellectual property, Tan et al. proposed a novel global similarity measurement for physical circuit designs [30].

In this paper, we analyze the correlations between circuit performance and the complex network characteristics of the physical design of integrated circuits, and explore the strength of the correlations with placement and routing. The transition of correlations from placement to routing is also studied in this context.

The paper is organized as follows. It introduces the fundamental characteristic related to weighted complex networks in the second section, conducts experiment schemes and analyze results in the third section, and concludes in the fourth section.

II. WEIGHTED COMPLEX NETWORK

In this section, we introduce a few fundamental concepts used in the analysis of weighted complex networks. A network or graph is usually represented by an adjacency matrix $\boldsymbol{A}$; element a_{ij} is set to 1 if there exists an edge connecting vertex $\boldsymbol{i}$ to vertex $\boldsymbol{j}$, and 0 otherwise. Similarly, a weighted network can also be described by a matrix $\boldsymbol{W}$ in which entry w_{ij} indicates the weight on the edge connecting vertex $\boldsymbol{i}$ and vertex $\boldsymbol{j}$ ($\mathrm{w}_{ij} = 0$ if the nodes $\boldsymbol{i}$ and $\boldsymbol{j}$ are not connected). In this context, we only consider the case of symmetric weight, namely, $\mathrm{w}_{ij} = \mathrm{w}_{ji}$. The weight can be categorized into dissimilarity weight and similarity weight. The dissimilarity weight is proportional to the distance, while the similarity weight is inversely proportional to the distance.

A. DEGREE AND STRENGTH

In a complex network, the most commonly utilized characteristic parameter is degree, which is defined as the number k_i of neighbors. The average degree of a network $< k >$ is defined as the average number of degrees of all nodes in the network, as shown by the following formula:

$$< k >= \frac{1}{N} \sum_{i=1}^{N} k_i \tag{1}$$

In contrast with vertex degree k_i, the vertex strength S_i used in the weighted network defines the significant property of the vertex and is given by the following:

$$S_i = \sum_{j \in N_i} w_{ij} \tag{2}$$

B. WEIGHTED CLUSTERING

The local structure of unweighted networks can be characterized by the number of times a subgraph appears in the network. The clustering coefficient, reflecting the local configuration of triangles, can be considered as a special case of this approach. Onnela et al. introduced subgraph intensity as the geometric mean of link weights and coherence as the ratio of the geometric to the corresponding arithmetic mean [31]. A natural generalization of clustering coefficient in the case of weighted networks (the so-called weighted clustering coefficient) is defined as follows:

$$C_{O,i}^{w} = \frac{1}{k_i (k_i - 1)} \sum_{j,k} \left(w_{ij}^{n} \cdot w_{jk}^{n} \cdot w_{ki}^{n} \right)^{\frac{1}{3}} \tag{3}$$

The average clustering coefficient $C = \frac{1}{N} \sum_{i=1}^{N} C_{O,i}^{w}$ expresses the statistical level of cohesiveness when measuring the global density of interconnected vertex triplets in the weighted network.

C. DISTANCE AND BETWEENNESS

The distance d_{ij} between two nodes in unweighted networks is defined as the minimum number of edges spanning from node $\boldsymbol{i}$ to node $\boldsymbol{j}$. Similarly, distance d_{ij} in a weighted network is represented as the sum of the weights of the shortest paths between node $\boldsymbol{i}$ and node $\boldsymbol{j}$.

The average distance L shown in the following formula represents the average degree of separation between nodes in the network:

$$L = \frac{2}{N (N - 1)} \sum_{i=1}^{N} \sum_{j=i+1}^{N} d_{ij} \tag{4}$$

Betweenness is another important centrality measure based on shortest paths and is defined as follows:

$$B_i = \sum_{j \neq l \neq i} \frac{N_{jl} (i)}{N_{jl}}. \tag{5}$$

where N_{jl} represents the number of shortest paths between nodes v_j and v_l, and $N_{jl}(\boldsymbol{i})$ represents the number of shortest paths passing through node v_i between node v_j and v_l. In a sense, betweenness reflects the influence of a node over the spread of information through the network.

III. EXPERIMENT

A. EXPERIMENT SCHEME

In the experiment, we use a Lenovo workstation platform with a 2.20 GHz CPU and 16.00GB memory. The operating system is Red Hat Enterprise Linux 6. A number of EDA tools are used for comparison. For instance, circuit format conversion tool DATC RDF [32]; placement tools Capo10.0 [33], Fastplace3 [34], Dragon3.0 [35], MPL6 [36], NTUplace3 [37], and FengShui2.6 [38]; routing tools BoxRoute2.0 [39], FGR [40], NCTU-GR2.0 [41], and NTHU-Route2.0 [42]; and complex network modeling and analysis tools MATLAB, PAJEK, and R.

We use the benchmark suite TAU 2017 Benchmark for the experiment. This benchmark originated for the timing contest [43]. It includes 17 circuits which will be run and

TABLE 1. The number of modules and nets in each circuit in TAU 2017 Benchmark.

Number	Benchmarks	Nets	Modules
1	ac97_ctrl	8683	8898
2	aes_core	16055	16185
3	b19_iccad	118612	118637
4	des_perf	95748	96323
5	des_perf_ispd	104413	104553
6	fft_ispd	45860	47844
7	matrix_mult_ispd	176890	178490
8	mgc_edit_dist_iccad	129039	129051
9	mgc_matrix_mult_iccad	176807	178407
10	pci_bridge32	14784	15063
11	systemcaes	7363	7492
12	systemcdes	3296	3361
13	tv80	5306	5338
14	usb_funct	12181	12303
15	usb_phy_ispd	469	488
16	vga_lcd_iccad	90919	91018
17	wb_dma	3524	3739

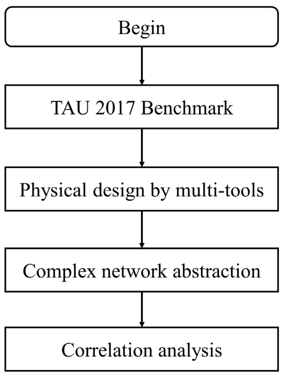

FIGURE 1. The experiment scheme.

analyzed by the previously mentioned tools. The number of nets ranges from 469 to 176,890, and the number of modules in the benchmark ranges from 488 to 178,490. The detailed information of the benchmark is listed in Table 1.

The experiment scheme is outlined in Figure 1. We place and route circuits in TAU 2017 Benchmark in the phase of ''physical design by multi-tools'', placements and layouts with different performance are obtained due to different p/l tools. In the phase of ''complex network abstraction'', placements and layouts of the circuits are transformed into weighted networks to extract characteristics parameters. In correlation analysis, the Pearson correlation coefficient is computed to evaluate the correlation between circuit performance and characteristic parameters.

1) PHYSICAL DESIGN BY MULTI-TOOLS

In the physical design, circuits in the benchmark are placed and routed to obtain designs with different performances. The designs will be used to form complex networks to extract various characteristics in the next phase.

First, we run the DATC circuit format conversion tool to convert the benchmark circuit into bookshelf format. Then

TABLE 2. Kruskal-Wallis test on correlations.

p-value	<S>	B	D	C
Placement	2.09 e-12	2.85 e-14	3.06 e-13	1.49 e-13
Routing	1.57 e-05	5.87 e-08	2.35 e-07	0.2014

the placement tools (i.e., Capo10.0, Fastplace3, Dragon3.0, MPL6, NTUplace3, and FengShui2.6) are completed to obtain placement designs of the circuits. The performances of the resulting placements may differ from each other due to the qualities of the tools. In the end, we also run the routing tools (i.e., BoxRoute2.0, FGR, NCTU-GR2.0, and NTHU-Route2.0) to obtain different layout designs.

2) COMPLEX NETWORK ABSTRACTION

In this phase, we first convert the formed placement into the weighted complex network. In each circuit placement, modules are regarded as nodes, and links between modules are regarded as edges. The weight of the edge between two connected nodes is approximated as the half-perimeter wire-length (HPWL) of the bounding box. The average strength, betweenness, average distance and clustering coefficient of the weighted complex network are also extracted by the analysis tools.

After the placement designs are routed, the structure of the layout design becomes clear and concrete. The nodes in the layout design are connected by horizontal and/or vertical links. Unlike placement, virtual nodes such as vias are added into the layout design. We use the nodes (include virtual nodes) and links to form complex networks. The average strength, betweenness, average distance and clustering coefficient of the weighted complex network are extracted by the analysis tools.

B. EXPERIMENTAL RESULTS AND ANALYSIS

In this section, we introduce the correlation analysis method and analyze the correlations of both placement design and layout design.

1) CORRELATION ANALYSIS

In correlation analysis, we use the Pearson correlation coefficient to compute the correlation between circuit performance and characteristic parameters. The coefficient is defined according to the following formula:

$$r = \frac{N\sum x_i y_i - \sum x_i \sum y_i}{\sqrt{N\sum x_i^2 - \left(\sum x_i\right)^2}\sqrt{N\sum y_i^2 - \left(\sum y_i\right)^2}} \tag{6}$$

where N is the number of total nodes, and x_i and y_i display two data series, where one indicates the circuit performance and another represents the characteristic parameter of the complex network.

When the correlation coefficient r is larger than 0, the two data series are positively correlated. In contrast, when r is smaller than 0, the correlation is negative. When r is equal to (or approximately) 0, it is uncorrelated.

TABLE 3. Correlation between average strength and circuit performance under different placement tools.

benchmark	Capo		Dragon		FastPlace		FengShui		MPL		NTUPlace	
	<S>	HPWL	<S>	HPWL	<S>	HPWL	<S>	HPWL	<S>	HPWL	<S>	HPWL
1	617.53	861963	628.00	1030686	762.78	1155152	616.30	1009685	503.57	796871	657.94	930814
2	530.94	1472879	607.59	1544510	701.77	1662166	610.86	1639811	475.44	1353533	584.65	1467712
3	473.27	8827399	499.10	9655616	529.46	10469994	482.96	9143570	404.24	8648192	478.52	8892596
4	1285.40	9040330	1090.00	9632846	1308.20	10765400	943.63	10705096	1403.00	8769532	1256.30	9650262
5	901.15	8043061	893.50	8485085	1148.00	9249793	858.30	8543042	1491.20	7654281	1104.50	8878770
6	1976.60	13054034	1939.60	12846118	1741.10	12115411	2215.80	14300138	1803.10	12115411	1848.80	12678131
7	1118.30	28463022	1154.80	28797712	1107.30	27241163	1878.20	41443730	1018.20	27178014	1137.20	26989704
8	1793.80	32597907	1753.60	35828582	1761.70	33367328	2553.20	42058959	1431.80	33460996	1792.30	34108207
9	1094.20	28087879	1169.30	28887903	1112.40	27339050	1888.90	41418269	1019.20	27199916	1137.50	27000081
10	508.76	1408642	485.24	1573577	663.05	1829865	606.53	1750255	385.11	1334155	542.39	1484578
11	800.02	1143442	754.70	1175582	887.34	1429369	1188.70	1460214	628.19	1061616	783.28	1161302
12	491.64	361362	486.22	381152	730.15	464669	700.20	428860	415.54	329909	497.22	355832
13	451.52	403401	492.96	467020	641.18	608193	546.52	508939	407.91	359326	483.03	415370
14	604.59	1230203	585.14	1323573	625.15	1394876	813.41	1529491	464.43	1139692	683.72	1355674
15	219.31	21907	261.01	27095	336.01	33382	278.13	28256	183.45	17486	243.71	23067
16	2008.40	15037538	1920.70	16478944	2034.60	18153323	2612.90	18801235	1640.90	15352642	1914.30	15304497
17	698.37	692932	679.00	707314	727.80	825425	937.65	831999	552.24	638884	656.63	701733
correlation	0.68023		0.71861		0.68531		0.78013		0.62986		0.71844	

TABLE 4. Correlation analysis between betweenness and performance under different placement tools.

benchmark	Capo		Dragon		FastPlace		FengShui		MPL		NTUPlace	
	B	HPWL	B	HPWL	B	HPWL	B	HPWL	B	HPWL	B	HPWL
1	75436	861963	72194	1030686	69337	1155152	69752	1009685	73315	796871	74593	930814
2	162509	1472879	162643	1544510	177838	1662166	161670	1639811	145768	1353533	170571	1467712
3	2181120	8827399	2214810	9655616	2002758	10469994	2035326	9143570	1604363	8648192	2019331	8892596
4	1465882	9040330	1393435	9632846	1403353	10765400	1354908	10705096	1391455	8769532	1468980	9650262
5	1511063	8043061	1517384	8485085	1530560	9249793	1890905	8543042	1364227	7654281	1552340	8878770
6	589561	13054034	592620	12846118	541868	12115411	561896	14300138	496082	12115411	586303	12678131
7	3856596	28463022	3384273	28797712	3363263	27241163	3397740	41443730	2870295	27178014	3691230	26989704
8	1357901	32597907	1332811	35828582	1307811	33367328	1332310	42058959	1100093	33460996	1341340	34108207
9	3544064	28087879	3505212	28887903	3455529	27339050	3437196	41418269	2879984	27199916	3633923	27000081
10	138317	1408642	131767	1573577	134932	1829865	135001	1750255	119728	1334155	137162	1484578
11	48565	1143442	46651	1175582	45568	1429369	47477	1460214	40762	1061616	46094	1161302
12	16982	361362	16878	381152	16672	464669	16838	428860	15281	329909	17031	355832
13	30966	403401	31326	467020	29543	608193	31267	508939	27603	359326	30961	415370
14	98329	1230203	98125	1323573	96771	1394876	94801	1529491	87406	1139692	102605	1355674
15	2045	21907	1964	27095	2136	33382	2112	28256	2056	17486	2095	23067
16	904629	15037538	901644	16478944	972423	18153323	944081	18801235	785185	15352642	990981	15304497
17	20496	692932	20132	707314	19131	825425	20282	831999	18743	638884	20372	701733
correlation	0.79586		0.76652		0.78811		0.78120		0.75062		0.75874	

2) CORRELATION IN PLACEMENT

In the experiment, we show the characteristic parameters and circuit performance under different placement tools for TAU 2017 Benchmark. The characteristic parameters and circuit performance (shown as HPWL) present differences due to the efficiencies of the tools. The performance of placement optimized by MPL is the best, followed by Capo, NTUPlace, Dragon, FastPlace, and FengShui. According to the resulting placement of each circuit, characteristic parameters of the corresponding complex network are calculated. The results are listed in Table 3 to Table 6. The correlations between circuit performance and characteristic parameters are calculated and shown in the last lines of the tables.

Table 3 shows values of different average strength $<S>$ and circuit performance under different placement tools. The correlations between circuit performance and average strength for different placement tools are 0.68023, 0.71861, 0.68531, 0.78013, 0.62986, and 0.71844. In Figure 2, the scatters illustrate the variation of average strength $<S>$ with HPWL for different placement tools. It can be observed that lower performance of the placement tool correlates with higher average strength.

Table 4 shows values of different betweenness B and circuit performance under different placement tools. The correlations between circuit performance and betweenness for different placement tools are 0.79586, 0.76652, 0.78811, 0.78120, 0.75062, and 0.75874. In Figure 3, the scatters illustrate variations of betweenness B with HPWL of different placement tools. The data roughly show that lower performance of the placement tool correlates with lower betweenness (except for MPL).

Table 5 shows values of different average distance D and circuit performance under different placement tools. The correlations between circuit performance and average distance

TABLE 5. Correlation analysis between average distance and performance under different placement tools.

benchmark	Capo		Dragon		FastPlace		FengShui		MPL		NTUPlace	
	D	HPWL	D	HPWL	D	HPWL	D	HPWL	D	HPWL	D	HPWL
1	1971.98	861963	1429.97	1030686	2369.05	1155152	1665.02	1009685	1337.53	796871	1750.45	930814
2	1122.15	1472879	1221.99	1544510	2024.75	1662166	1576.08	1639811	1026.03	1353533	1462.11	1467712
3	2754.29	8827399	3913.79	9655616	4386.03	10469994	4097.44	9143570	2756.37	8648192	3185.25	8892596
4	4731.69	9040330	3158.55	9632846	4339.80	10765400	3759.77	10705096	3440.86	8769532	3947.78	9650262
5	2732.58	8043061	2908.44	8485085	4031.44	9249793	3799.22	8543042	2872.70	7654281	3884.50	8878770
6	3572.48	13054034	3735.26	12846118	4818.87	12115411	2886.28	14300138	4020.55	12115411	3570.71	12678131
7	5584.80	28463022	5102.61	28797712	5956.05	27241163	4669.19	41443730	5423.96	27178014	5301.78	26989704
8	2503.98	32597907	2645.89	35828582	2798.41	33367328	3732.66	42058959	2491.75	33460996	2960.68	34108207
9	5765.77	28087879	5245.85	28887903	5943.51	27339050	4575.51	41418269	5430.66	27199916	5381.28	27000081
10	1343.31	1408642	1374.45	1573577	2238.67	1829865	1799.51	1750255	1207.57	1334155	1759.07	1484578
11	872.39	1143442	878.03	1175582	1213.03	1429369	1197.70	1460214	816.57	1061616	943.75	1161302
12	613.47	361362	631.72	381152	976.41	464669	818.77	428860	544.63	329909	630.79	355832
13	568.43	403401	604.83	467020	856.01	608193	798.47	508939	528.84	359326	610.62	415370
14	1202.20	1230203	1268.06	1323573	1510.97	1394876	1461.32	1529491	1037.22	1139692	1395.08	1355674
15	410.35	21907	437.98	27095	645.99	33382	397.03	28256	313.76	17486	471.38	23067
16	2805.28	15037538	4350.86	16478944	4779.10	18153323	3756.60	18801235	2979.34	15352642	3060.31	15304497
17	913.44	692932	956.22	707314	1226.84	825425	1086.09	831999	775.68	638884	959.50	701733
correlation	0.77501		0.78489		0.73827		0.78911		0.79854		0.77627	

TABLE 6. Correlation analysis between clustering coefficient and performance under different placement tools.

benchmark	Capo		Dragon		FastPlace		FengShui		MPL		NTUPlace	
	C	HPWL	C	HPWL	C	HPWL	C	HPWL	C	HPWL	C	HPWL
1	0.0987	861963	0.1321	1030686	0.1517	1155152	0.0932	1009685	0.0863	796871	0.0875	930814
2	0.0026	1472879	0.0036	1544510	0.0017	1662166	0.0025	1639811	0.0029	1353533	0.0037	1467712
3	0.0559	8827399	0.0616	9655616	0.0931	10469994	0.0595	9143570	0.0493	8648192	0.0576	8892596
4	0.0017	9040330	0.0015	9632846	0.0009	10765400	0.0013	10705096	0.0016	8769532	0.0014	9650262
5	0.0012	8043061	0.0013	8485085	0.0010	9249793	0.0010	8543042	0.0014	7654281	0.0010	8878770
6	0.1454	13054034	0.1554	12846118	0.0910	12115411	0.1297	14300138	0.1826	12115411	0.1423	12678131
7	0.0230	28463022	0.0311	28797712	0.0188	27241163	0.0224	41443730	0.0247	27178014	0.0244	26989704
8	0.0346	32597907	0.0397	35828582	0.0514	33367328	0.0354	42058959	0.0382	33460996	0.0330	34108207
9	0.0234	28087879	0.0302	28887903	0.0178	27339050	0.0225	41418269	0.0253	27199916	0.0244	27000081
10	0.0400	1408642	0.0412	1573577	0.0528	1829865	0.0378	1750255	0.0389	1334155	0.0347	1484578
11	0.1024	1143442	0.1256	1175582	0.1996	1429369	0.0825	1460214	0.1675	1061616	0.1096	1161302
12	0.0019	361362	0.0020	381152	0.0027	464669	0.0015	428860	0.0019	329909	0.0017	355832
13	0.0666	403401	0.0757	467020	0.1206	608193	0.0686	508939	0.0831	359326	0.0691	415370
14	0.1028	1230203	0.1039	1323573	0.1245	1394876	0.1045	1529491	0.0988	1139692	0.0929	1355674
15	0.1070	21907	0.1318	27095	0.1864	33382	0.1054	28256	0.1152	17486	0.1076	23067
16	0.3408	15037538	0.4250	16478944	0.7080	18153323	0.3665	18801235	0.3988	15352642	0.3295	15304497
17	0.0570	692932	0.0547	707314	0.0904	825425	0.0496	831999	0.0376	638884	0.0488	701733
correlation	0.00413		0.02595		0.04227		0.00199		0.02922		0.01134	

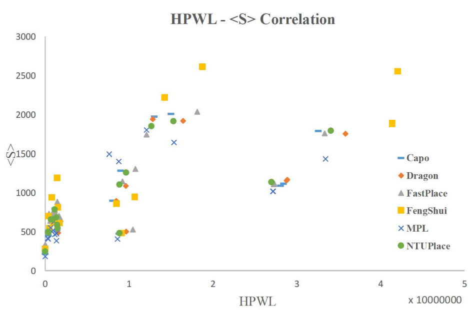

FIGURE 2. The HPWL-<S> correlation in placement for TAU 2017 Benchmark.

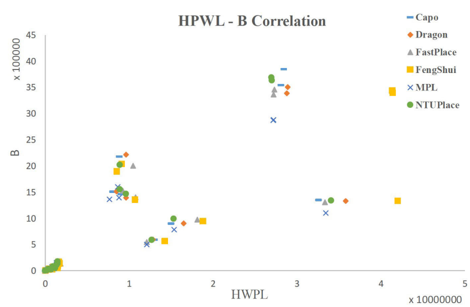

FIGURE 3. The HPWL-B correlation in placement for TAU 2017 Benchmark.

for different placement tools are 0.77501, 0.78489, 0.73827, 0.78911, 0.79854, and 0.77627. In Figure 4, the scatters illustrate the variation of average distance D with HPWL of different placement tools. The data roughly show that lower performance of the placement tool correlates with higher average distance.

Table 6 shows values of different clustering coefficient C and circuit performance under different placement tools. The

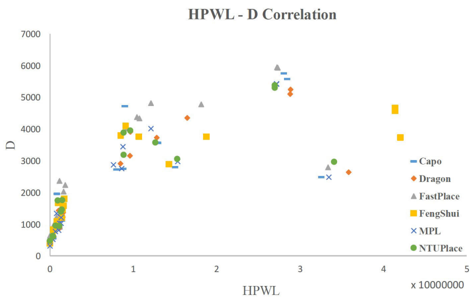

FIGURE 4. **The HPWL-D correlation in placement for TAU 2017 Benchmark.**

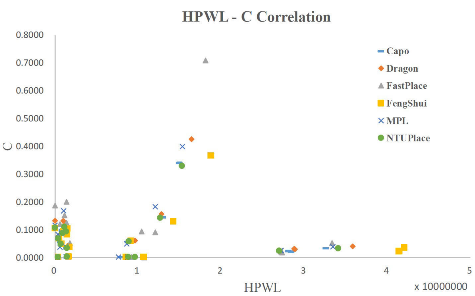

FIGURE 5. **The HPWL-C correlation in placement for TAU 2017 Benchmark.**

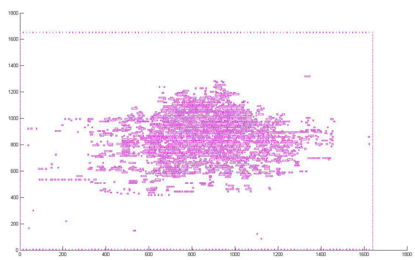

FIGURE 6. **The placement of wb_dma by NTUPlace3.**

correlations between circuit performance and clustering coefficient for different placement tools are 0.00413, 0.02595, 0.04227, 0.00199, 0.02922, and 0.01134. In Figure 5, the scatters illustrate the variation of clustering coefficient C with HPWL for different placement tools. The data roughly show that lower performance of the placement tool correlates with higher clustering coefficient (except for FengShui).

We show the placement of the wb_dma circuit in Figure 6 and illustrate the three-dimensional weighted complex network of the circuit in Figure 7.

The correlations between circuit performance of placement and characteristic parameters are listed in the last lines of Table 3 to Table 6. The correlation between circuit performance and average strength averages 0.70210, the correlation between circuit performance and betweenness averages 0.77351, the correlation between circuit performance and average distance averages 0.77702, and the correlation between circuit performance and clustering

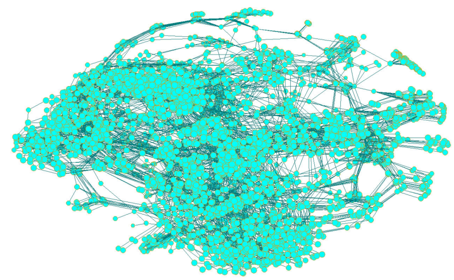

FIGURE 7. **The weighted complex network of placement of wb_dma.**

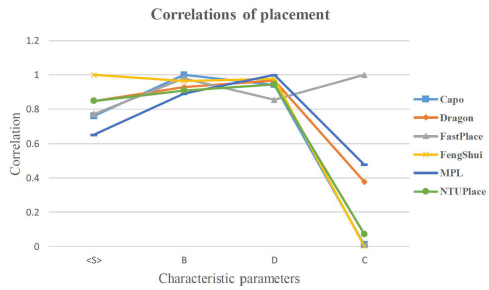

FIGURE 8. **Correlation comparison for different placement tools.**

coefficient is 0.01911. The correlations are illustrated in Figure 8. The data show that circuit performance has the strongest correlation with average distance, followed by betweenness and average strength, and has the weakest correlation with th clustering coefficient.

3) CORRELATION IN LAYOUT

In this section, it shows the characteristic parameters and circuit performance under different route tools for TAU 2017 Benchmark. The characteristic parameters and circuit performance (shown as WL) present differences due to the efficiencies of the tools. The layout performance generated by NTHU is the best, those of NCTU-GR and BoxRouter are nearly identical and that of FGR is the worst. We convert the layout design into a complex network and calculate the corresponding characteristic parameters. The correlations between the circuit performance of the layout and characteristic parameters are calculated and shown in the last lines of Table 7 to Table 10.

Table 7 shows values of different average strength $<S>$ and circuit performance under different routing tools. The correlations between WL and average strength for different routing tools are 0.50221, 0.54040, 0.48427, and 0.16201. In Figure 9, the scatters illustrate the variation of average strength $<S>$ with WL for different route tools. This shows that lower performance of the routing tool correlates with higher average strength.

Table 8 shows values of different betweenness B and circuit performance under different routing tools. The correlations between WL and betweenness for different routing tools are 0.87639, 0.91437, 0.88974, and 0.96254. In Figure 10, the

TABLE 7. Correlation analysis between average strength and performance under different routing tools.

benchmark	BoxRouter		FGR		NCTU-GR		NTHU	
	<S>	WL	<S>	WL	<S>	WL	<S>	WL
1	7.58	45754	10.44	45594	6.76	44688	6.93	44728
2	19.15	121430	31.41	129339	19.85	124862	18.14	128194
3	30.63	770772	50.62	772523	29.57	758380	26.23	718138
4	12.22	484159	18.47	484307	11.49	485923	11.46	477643
5	14.56	500633	23.08	498642	13.66	497758	13.59	491412
6	9.52	400461	13.29	400809	8.75	400494	8.93	395864
7	16.12	1238533	24.91	1272274	15.53	1238411	14.71	1231382
8	22.46	1702299	37.07	1702773	23.18	1811269	13.56	1314700
9	16.50	1227651	25.47	1241819	15.89	1253943	15.04	1241869
10	8.76	71013	12.26	70666	7.80	69948	8.04	70103
11	15.86	62396	22.22	65656	14.80	61461	13.54	58239
12	15.35	23324	21.614	24116	14.21	23252	13.38	23180
13	20.88	32934	35.89	34412	22.21	32976	22.65	30364
14	13.08	85960	19.69	96117	12.11	86214	11.45	88358
15	5.46	1381	7.55	1353	5.24	1338	5.34	1338
16	21.15	1327184	35.25	1263917	19.90	1457962	11.40	1019340
17	11.71	32020	16.76	30864	10.98	30807	11.15	30817
correlation	0.50221		0.54040		0.48427		0.16201	

TABLE 8. Correlation analysis between average betweenness and performance under different routing tools.

benchmark	BoxRouter		FGR		NCTU-GR		NTHU	
	B	WL	B	WL	B	WL	B	WL
1	41400	45754	41001	45594	36655	44688	34327	44728
2	68597	121430	60266	129339	56321	124862	60976	128194
3	446864	770772	349096	772523	324789	758380	303465	718138
4	379964	484159	382195	484307	363319	485923	346899	477643
5	361320	500633	331415	498642	323393	497758	317124	491412
6	158120	400461	165050	400809	158200	400494	149384	395864
7	594716	1238533	547009	1272274	498976	1238411	515488	1231382
8	432625	1702299	507777	1702773	422771	1811269	415626	1314700
9	578686	1227651	553575	1241819	507101	1253943	519732	1241869
10	63212	71013	58747	70666	56000	69948	52822	70103
11	21747	62396	22929	65656	17244	61461	16703	58239
12	9186	23324	10164	24116	8429	23252	8636	23180
13	10827	32934	8780	34412	7980	32976	6823	30364
14	43124	85960	41026	96117	34464	86214	36453	88358
15	1556	1381	966	1353	1055	1338	1054	1338
16	361796	1327184	344079	1263917	327186	1457962	415266	1019340
17	12357	32020	10980	30864	10011	30807	9575	30817
correlation	0.87639		0.91437		0.88974		0.96254	

scatters illustrate the variation of betweenness B with WL for different route tools. This roughly shows that lower performance of the routing tool correlates with higher betweenness (except for BoxRouter).

Table 9 shows values of different average distance D and circuit performance under different routing tools. The correlations between WL and average distance for different routing tools are 0.19266, 0.28472, 0.25067, and 0.55930. In Figure 11, the scatters illustrate the variation of average distance D with WL for different routing tools. This roughly shows that lower performance of the routing tool correlates with lower average distance.

Table 10 shows the values of different clustering coefficient C and circuit performance under different routing tools. The correlations between WL and clustering coefficient for different routing tools are 0.46342, -0.33941, 0.44012, and 0.10439. Notably, the correlation between clustering coefficient and circuit performance for FGR is negative. In Figure 12, the scatters illustrate the variation of clustering coefficient C with WL for different routing tools. For the NTHU, NCTU-GR and BoxRouter tools, it shows that higher performance of the routing tool correlates with lower clustering coefficient. The FGR tool presents a different style due to the negative correlation.

It shows the layout of the wb_dma circuit generated by FGR in Figure 13 and illustrates the three-dimensional weighted complex network of the circuit in Figure 14.

The correlations between layout circuit performance and the characteristic parameters are listed in the last lines of Table 7 to Table 10. The correlation between circuit performance and average strength averages 0.42222, the correlation between circuit performance and betweenness averages 0.91076, the correlation between circuit performance and average distance averages 0.32184, and the correlation

TABLE 9. Correlation analysis between average distance and performance under different routing tools.

benchmark	BoxRouter		FGR		NCTU-GR		NTHU	
	D	WL	D	WL	D	WL	D	WL
1	7.07	45754	7.14	45594	7.61	44688	7.23	44728
2	4.60	121430	4.37	129339	4.43	124862	4.74	128194
3	4.35	770772	4.49	772523	4.90	758380	5.40	718138
4	9.04	484159	9.07	484307	9.53	485923	9.21	477643
5	8.87	500633	8.20	498642	8.83	497758	8.59	491412
6	6.03	400461	5.81	400809	6.58	400494	6.34	395864
7	6.57	1238533	6.28	1272274	6.70	1238411	6.83	1231382
8	4.99	1702299	5.51	1702773	5.46	1811269	6.69	1314700
9	6.48	1227651	6.25	1241819	6.75	1253943	6.76	1241869
10	6.90	71013	6.64	70666	7.11	69948	6.66	70103
11	3.56	62396	3.93	65656	3.65	61461	3.88	58239
12	3.61	23324	4.12	24116	4.11	23252	4.08	23180
13	2.70	32934	2.52	34412	2.49	32976	2.39	30364
14	4.87	85960	4.82	96117	5.03	86214	5.08	88358
15	5.82	1381	3.65	1353	4.05	1338	4.06	1338
16	5.24	1327184	5.44	1263917	5.69	1457962	8.43	1019340
17	3.79	32020	3.84	30864	4.10	30807	3.92	30817
correlation	0.19266		0.28472		0.25067		0.55930	

TABLE 10. Correlation analysis between clustering coefficient and performance under different routing tools.

benchmark	BoxRouter		FGR		NCTU-GR		NTHU	
	C	WL	C	WL	C	WL	C	WL
1	0.0518	45754	0.0066	45594	0.0453	44688	0.0570	44728
2	0.1108	121430	0.0216	129339	0.0898	124862	0.0790	128194
3	0.1729	770772	0.0203	772523	0.1279	758380	0.1040	718138
4	0.0624	484159	0.0088	484307	0.0641	485923	0.0661	477643
5	0.0748	500633	0.0111	498642	0.0708	497758	0.0752	491412
6	0.0654	400461	0.0069	400809	0.0638	400494	0.0682	395864
7	0.1033	1238533	0.0093	1272274	0.0950	1238411	0.0925	1231382
8	0.1330	1702299	0.0092	1702773	0.1155	1811269	0.0685	1314700
9	0.1046	1227651	0.0092	1241819	0.0957	1253943	0.0938	1241869
10	0.0516	71013	0.0059	70666	0.0524	69948	0.0548	70103
11	0.1160	62396	0.0167	65656	0.0961	61461	0.0833	58239
12	0.1091	23324	0.0213	24116	0.0757	23252	0.0640	23180
13	0.1101	32934	0.0205	34412	0.1126	32976	0.1015	30364
14	0.0939	85960	0.0106	96117	0.0791	86214	0.0700	88358
15	0.0184	1381	0.0077	1353	0.0193	1338	0.0223	1338
16	0.1224	1327184	0.0081	1263917	0.0947	1457962	0.0471	1019340
17	0.0703	32020	0.0120	30864	0.0796	30807	0.0718	30817
correlation	0.46342		-0.33941		0.44012		0.10439	

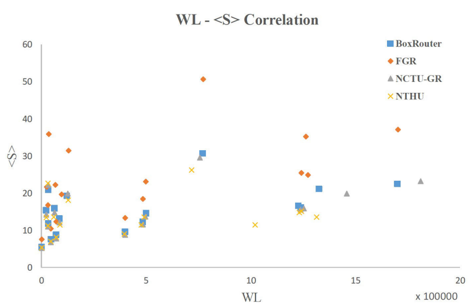

FIGURE 9. The WL-<S> layout correlation for TAU 2017 Benchmark.

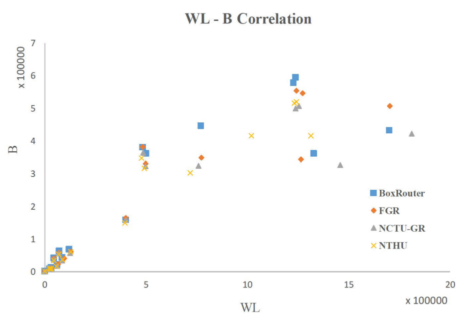

FIGURE 10. The WL-B layout correlation for TAU 2017 Benchmark.

between circuit performance and clustering coefficient is 0.16713. The correlations are illustrated in Figure 15. The data show that layout circuit performance has the strongest correlation with betweenness, followed by average strength and average distance, and has the weakest correlation with the clustering coefficient.

In Figure 16, we show the transition of correlations between circuit performance and characteristic parameters

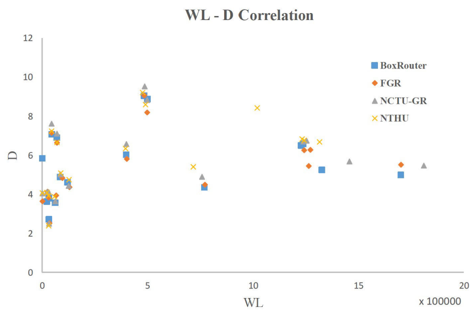

FIGURE 11. The WL-D layout correlation for TAU 2017 Benchmark.

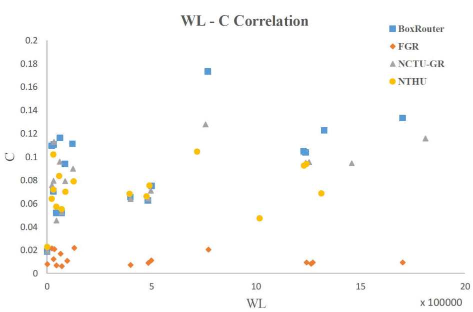

FIGURE 12. The WL-C layout correlation for TAU 2017 Benchmark.

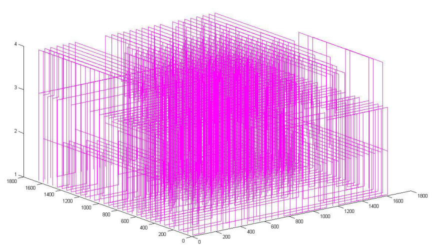

FIGURE 13. The layout of wb_dma by FGR.

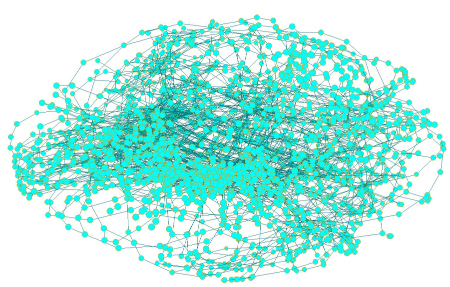

FIGURE 14. The weighted complex layout network of wb_dma.

from placement to routing. The orange curve presents the correlation between circuit performance and characteristic parameters in placement, while the blue curve presents the correlation between circuit performance and characteristic parameters in route. After routing, the correlations between circuit performance and average distance and average strength have been weakened, while the correlations between circuit performance and betweenness and clustering

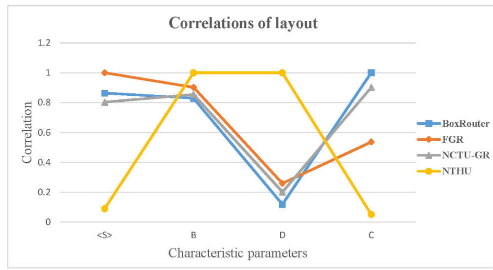

FIGURE 15. Correlation comparison for different routing tools.

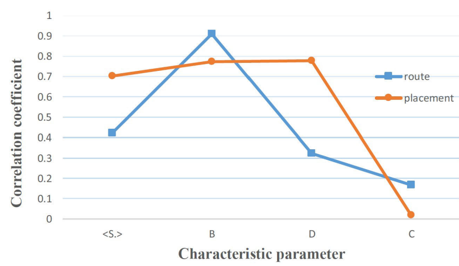

FIGURE 16. Correlation change from placement to routing.

coefficient have been strengthened. Notably, the correlation between circuit performance and betweenness has been further strengthened after routing, and it presents a remarkable difference in comparison with other characteristic parameters.

We had a statistical analysis on the experimental data using the Kruskal-Wallis test. As shown in Table 2, there are extreme significant correlations between circuit performance and characteristic parameters (p-value < 0.0001), except no significant correlation between circuit performance and clustering coefficient in routing (p-value > 0.05). The conclusion is consistent with the results shown in Figure 2 - Figure 12.

IV. CONCLUSION

In this paper, we have conducted a study regarding the case of characteristic parameters and circuit performance under different placement and routing tools. The experimental results of TAU 2017 Benchmark show that circuit performance varies due to the efficiencies of the optimization tools. The qualities of the placement tools ranked from best to worst are MPL, Capo, NTUPlace, Dragon, FastPlace, and Feng-Shui; the ranked qualities of the routing tools are NTHU, NCTU-GR, BoxRouter, and FGR. The strength of the correlations between circuit performance and the complex network characteristics in placement follows the order of average distance, betweenness, average strength, and the clustering coefficient; the strength of the correlations with routing follows the order of betweenness, average strength, average distance, and the clustering coefficient. We also show the transition of the correlations from placement to routing. After routing, the correlations between circuit performance, average distance and average strength have been weakened, while the correlations between circuit performance, betweenness and the clustering coefficient have been strengthened. Notably, the correlation between circuit performance and betweenness has been further strengthened after routing, which presents a remarkable difference in comparison with other characteristic parameters.

REFERENCES

[1] H. N. Khan, D. A. Hounshell, and E. R. H. Fuchs, "Publisher correction: Science and research policy at the end of Moore's law," *Nature Electron.*, vol. 1, no. 2, p. 146, Feb. 2018.
[2] A. B. Kahng, "New directions for learning-based IC design tools and methodologies," in *Proc. 23rd Asia South Pacific Design Automat. Conf. (ASP-DAC)*, Jan. 2018, pp. 405–410.
[3] A. Kahng, A. B. Kahng, H. Lee, and J. Li, "PROBE: A placement, routing, back-end-of-line measurement utility," *IEEE Trans. Comput.-Aided Design Integr. Circuits Syst.*, vol. 37, no. 7, pp. 1459–1472, Jul. 2018.
[4] B. Zhang, G. Huang, Z. Zheng, J. Ren, and C. Hu, "Approach to mine the modularity of software network based on the most vital nodes," *IEEE Access*, vol. 6, pp. 32543–32553, 2018.
[5] M. E. J. Newman, "The structure and function of complex networks," *SIAM Rev.*, vol. 45, no. 2, pp. 167–256, 2003.
[6] W. Guan, X. Wen, L. Wang, Z. Lu, and Y. Shen, "A service-oriented deployment policy of end-to-end network slicing based on complex network theory," *IEEE Access*, vol. 6, pp. 19691–19701, 2018.
[7] L. Wang, R. Song, Z. Qu, H. Zhao, and C. Zhai, "Study of China's publicity translations based on complex network theory," *IEEE Access*, vol. 6, pp. 35753–35763, 2018.
[8] E. L. C. da Silva, M. D. O. Rosa, K. V. O. Fonseca, R. Luders, and N. P. Kozievitch, "Combining K-means method and complex network analysis to evaluate city mobility," in *Proc. IEEE 19th Int. Conf. Intell. Transp. Syst. (ITSC)*, Nov. 2016, pp. 1666–1671.
[9] S. Supriya, S. Siuly, H. Wang, J. Cao, and Y. Zhang, "Weighted visibility graph with complex network features in the detection of epilepsy," *IEEE Access*, vol. 4, pp. 6554–6566, 2016.
[10] H. T. Nguyen, N. P. Nguyen, T. Vu, H. X. Hoang, and T. N. Dinh, "Transitivity demolition and the fall of social networks," *IEEE Access*, vol. 5, pp. 15913–15926, 2017.
[11] Z. Song, Y. Sun, H. Yan, D. Wu, P. Niu, and X. Wu, "Robustness of smart manufacturing information systems under conditions of resource failure: A complex network perspective," *IEEE Access*, vol. 6, pp. 3731–3738, 2018.
[12] D. J. Watts and S. H. Strogatz, "Collective dynamics of 'small-world'networks," *Nature*, vol. 393, pp. 440–442, 1998.
[13] R. F. I. Cancho and R. V. Solé, "Optimization in complex networks," in *Statistical Mechanics of Complex Networks*. Berlin, Germany: Springer, 2003, pp. 114–126.
[14] A. Santoro, V. Latora, G. Nicosia, and V. Nicosia, "Pareto optimality in multilayer network growth," *Phys. Rev. Lett.*, vol. 121, no. 12, Sep. 2018, Art. no. 128302.
[15] R. Albert, H. Jeong, and A.-L. Barabási, "Error and attack tolerance of complex networks," *Nature*, vol. 406, no. 6794, pp. 378–382, Jul. 2000.
[16] P. Holme, B. J. Kim, C. N. Yoon, and S. K. Han, "Attack vulnerability of complex networks," *Phys. Rev. E, Stat. Phys. Plasmas Fluids Relat. Interdiscip. Top.*, vol. 65, no. 5, May 2002, Art. no. 056109.
[17] T. Gavrilchenko and E. Katifori, "Resilience in hierarchical fluid flow networks," *Phys. Rev. E, Stat. Phys. Plasmas Fluids Relat. Interdiscip. Top.*, vol. 99, no. 1, Jan. 2019, Art. no. 012321.
[18] T. Nie, Z. Guo, K. Zhao, and Z.-M. Lu, "New attack strategies for complex networks," *Phys. A, Stat. Mech. Appl.*, vol. 424, pp. 248–253, Apr. 2015.
[19] Y.-Y. Liu, J.-J. Slotine, and A.-L. Barabási, "Controllability of complex networks," *Nature*, vol. 473, no. 7346, pp. 167–173, May 2011.
[20] T. Ryczkowski, A. Fronczak, and P. Fronczak, "How transfer flights shape the structure of the airline network," *Sci. Rep.*, vol. 7, no. 1, pp. 1–8, Dec. 2017.
[21] T. Verma, N. A. M. Araújo, and H. J. Herrmann, "Revealing the structure of the world airline network," *Sci. Rep.*, vol. 4, no. 1, pp. 5638–5649, May 2015.
[22] V. Latora and M. Marchiori, "Is the boston subway a small-world network?" *Phys. A, Stat. Mech. Appl.*, vol. 314, nos. 1–4, pp. 109–113, Nov. 2002.
[23] M. Li, H. Wang, and H. Wang, "Resilience assessment and optimization for urban rail transit networks: A case study of beijing subway network," *IEEE Access*, vol. 7, pp. 71221–71234, 2019.
[24] G. Ódor and B. Hartmann, "Heterogeneity effects in power grid network models," *Phys. Rev. E, Stat. Phys. Plasmas Fluids Relat. Interdiscip. Top.*, vol. 98, no. 2, pp. 022305–022314, Aug. 2018.
[25] R. F. I. Cancho, C. Janssen, and R. V. Solé, "The topology of technology graphs: Small world patterns in electronic circuits," *Phys. Rev. E, Stat. Phys. Plasmas Fluids Relat. Interdiscip. Top.*, vol. 64, no. 1, pp. 046119–046123, 2001.
[26] C. Teuscher, "Nature-inspired interconnects for self-assembled large-scale network-on-chip designs," *Chaos*, vol. 17, no. 2, Jun. 2007, Art. no. 026106.
[27] C. Teuscher, N. Gulbahce, and T. Rohlf, "Assessing random dynamical network architectures for nanoelectronics," in *Proc. IEEE Int. Symp. Nanosc. Architectures*, Jun. 2008, pp. 16–23.
[28] N. Oshida and S. Ihara, "Packet traffic analysis of scale-free networks for large-scale network-on-chip design," *Phys. Rev. E, Stat. Phys. Plasmas Fluids Relat. Interdiscip. Top.*, vol. 74, no. 2, Aug. 2006, Art. no. 026115.
[29] S. Zhan, J. F. Miller, and A. M. Tyrrell, "An evolutionary system using development and artificial genetic regulatory networks for electronic circuit design," *Biosystems*, vol. 98, no. 3, pp. 176–192, Dec. 2009.
[30] H. Tan, M. Peng, C. K. Tse, and F. Wu, "Global similarity tests of physical designs of circuits: A complex network approach," *Appl. Math. Comput.*, vol. 230, pp. 96–103, Mar. 2014.
[31] J.-P. Onnela, J. Saramäki, J. Kertész, and K. Kaski, "Intensity and coherence of motifs in weighted complex networks," *Phys. Rev. E, Stat. Phys. Plasmas Fluids Relat. Interdiscip. Top.*, vol. 71, no. 6, Jun. 2005, Art. no. 065103.
[32] J. Jung, I. H.-R. Jiang, J. Chen, S.-T. Lin, Y.-L. Li, V. N. Kravets, and G.-J. Nam, "DATC RDF: An open design flow from logic synthesis to detailed routing," 2018, *arXiv:1810.01078*. [Online]. Available: http://arxiv.org/abs/1810.01078
[33] J. A. Roy, S. N. Adya, D. A. Papa, and I. L. Markov, "Min-cut floorplacement," *IEEE Trans. Comput.-Aided Design Integr. Circuits Syst.*, vol. 25, no. 7, pp. 1313–1326, Jul. 2006.
[34] N. Viswanathan, M. Pan, and C. Chu, "FastPlace 3.0: A fast multilevel quadratic placement algorithm with placement congestion control," in *Proc. Asia South Pacific Design Automat. Conf.*, Jan. 2007, pp. 135–140.
[35] X. Yang, B.-K. Choi, and M. Sarrafzadeh, "Routability-driven white space allocation for fixed-die standard-cell placement," *IEEE Trans. Comput.-Aided Design Integr. Circuits Syst.*, vol. 22, no. 4, pp. 410–419, Apr. 2003.
[36] T. F. Chan, J. Cong, J. R. Shinnerl, K. Sze, and M. Xie, "mPL6: Enhanced multilevel mixed-size placement," in *Proc. Int. Symp. Phys. Design*, Apr. 2006, pp. 212–214.
[37] T.-C. Chen, Z.-W. Jiang, T.-C. Hsu, H.-C. Chen, and Y.-W. Chang, "NTUplace3: An analytical placer for large-scale mixed-size designs with preplaced blocks and density constraints," *IEEE Trans. Comput.-Aided Design Integr. Circuits Syst.*, vol. 27, no. 7, pp. 1228–1240, Jul. 2008.
[38] A. Khatkhate, C. Li, A. R. Agnihotri, M. C. Yildiz, S. Ono, C.-K. Koh, and P. H. Madden, "Recursive bisection based mixed block placement," in *Proc. Int. Symp. Phys. Design (ISPD)*, Apr. 2004, pp. 84–89.
[39] M. Cho, K. Lu, K. Yuan, and D. Z. Pan, "BoxRouter 2.0: Architecture and implementation of a hybrid and robust global router," in *Proc. IEEE/ACM Int. Conf. Comput.-Aided Design*, Nov. 2007, pp. 503–508.
[40] J. Hu, J. A. Roy, and I. L. Markov, "Completing high-quality global routes," in *Proc. 19th Int. Symp. Phys. Design (ISPD)*, Mar. 2010, pp. 35–41.
[41] W.-H. Liu, W.-C. Kao, Y.-L. Li, and K.-Y. Chao, "NCTU-GR 2.0: Multithreaded collision-aware global routing with bounded-length maze routing," *IEEE Trans. Comput.-Aided Design Integr. Circuits Syst.*, vol. 32, no. 5, pp. 709–722, May 2013.
[42] Y.-J. Chang, Y.-T. Lee, and T.-C. Wang, "NTHU-route 2.0: A fast and stable global router," in *Proc. IEEE/ACM Int. Conf. Comput.-Aided Design*, Nov. 2008, pp. 338–343.
[43] *Tau 2017 Benchmark*. Accessed: 2017. [Online]. Available: http://www.tauworkshop.com/2017/

TINGYUAN NIE (Member, IEEE) received the B.S. degree in computer science from the Wuhan University of Technology, in 1993, and the M.S. and Ph.D. degrees in computer engineering from Kochi University, Japan, in 2005 and 2008, respectively. He is currently a Professor with the School of Information and Control Engineering, Qingdao University of Technology, Qingdao, China. His research interests include very-large-scale integration CAD algorithms and IC security.

BO FAN received the B.S. degree from the School of Information and Control Engineering, Qingdao University of Technology, where he is currently pursuing the master's degree. His research interests include very-large-scale integration optimization and complex networks.

ZUYUAN ZHU photograph and biography not available at the time of publication.

LIJIAN ZHOU received the B.S. and M.S. degrees from the School of Computer and Information Technology, Northeast Petroleum University of Technology, in 1993 and 1996, respectively, and the Ph.D. degree in computer engineering from the Ocean University of China, in 2007. She is currently a Professor with the School of Information and Control Engineering, Qingdao University of Technology, China. Her research interests include image processing and watermarking methodology for IPP.